POLOIDAL FLUX REQUIREMENT: ANALYSIS AND APPLICATION TO THE IGNITOR CONFIGURATION

MAGNET SYSTEMS

KEYWORDS: *poloidal flux, volt second, compact tokamak*

MARCO NASSI *Massachusetts Institute of Technology*
77 Massachusetts Avenue, Cambridge, Massachusetts 02139

Received March 16, 1992
Accepted for Publication December 8, 1992

The definitions and correlations existing between different terms used by physicists and engineers are clarified in order to deal with the assessment of the poloidal flux requirement in a fusion experiment.

The theoretical formulation of both the Faraday and the Poynting methods, for the internal flux evaluation, is briefly reviewed. Heuristic expressions that allow estimates of internal flux consumption are reported for the specific case of an ignition experiment represented by the Ignitor configuration.

The analytical and heuristic results for both internal and external poloidal flux requirements are checked against numerical evaluations carried out by using the TSC transport and magnetohydrodynamics code and the TEQ equilibrium code. A fairly good agreement between the different estimates is found. This suggests that simple heuristic expressions can be used to evaluate the poloidal flux requirement of future experiments, even if a detailed simulation of the plasma current penetration process is strongly recommended to correctly assess and optimize the resistive poloidal flux consumption.

Finally, the poloidal flux requirement for different plasma scenarios in the Ignitor experiment is compared with the magnetic flux variation that can be delivered by the poloidal field system.

I. INTRODUCTION

The Ignitor tokamak[1-3] is designed to reach and investigate fusion burning conditions for deuterium-tritium (D-T) plasmas. To achieve this objective, the strategy involves an optimal combination of ohmic and alpha-particle heating.[4-6] Because of the importance of the ohmic heating, it is essential to be able to estimate the poloidal flux requirement of the current ramp and flattop phases of the discharge. The current ramp phase is the most poloidal flux consuming part of the discharge. Therefore, close attention must be paid to its analysis because a small error could result in a large contraction in the duration of the flattop phase if an adequate poloidal flux margin is not provided.

The problem of the evaluation of the poloidal flux required to induce a certain value of plasma current in a specific tokamak configuration can be solved by using magnetohydrodynamic (MHD) and transport codes such as TSC (Ref. 7) or WHIST (Ref. 8). The TSC code, for example, once the external coil positions, the desired plasma current, and the shape and position are provided as input, is able to model the plasma discharge, evaluating all the plasma parameters and profiles (for current, pressure, temperature, etc.), including the plasma poloidal flux requirement. This last quantity is due to an inductive term, which is proportional to the value of the magnetic energy stored in the plasma, and a resistive term, which is related to the energy dissipated during the plasma current penetration process. The code results clearly depend on the models assumed for the plasma resistivity and the diffusion coefficient for the plasma thermal energy. The good benchmarks of these codes against experimental data provided by several existing tokamaks have proven the accuracy of the models and of the numerical schemes used in the codes. On the other hand, these codes are complicated and consume large amounts of CPU time. Simpler and faster equilibrium codes, such as the TEQ code,[9] can be used to calculate the inductive part of the plasma poloidal flux requirement once the final plasma shape, position, and profiles for current and pressure have been assumed or evaluated with a transport code. The evaluation of the resistive part requires a time-dependent simulation of the plasma current profile evolution and, therefore, cannot be carried out by an equilibrium code. In recent years, heuristic analytical models for the inductive flux consumption have

been derived, and empirical scaling laws for the resistive requirement have been drawn from existing tokamak data. These simplified models have been extensively used to predict the poloidal flux requirement of future tokamak experiments.

In this paper, we present results for the Ignitor configuration obtained from the TSC and TEQ codes, and we check them against results provided by the heuristic models. This comparison is useful to verify the possibility of applying the heuristic models to a tokamak configuration that presents plasma parameters never achieved before. Furthermore, this double check of the poloidal flux requirement assumes particular importance in the Ignitor design because, as in the design of other high-field, compact tokamaks, the poloidal magnets are pushed close to their maximum allowable operating temperature to achieve an adequate flux swing to produce the desired plasma current and maintain it for a time interval adequate to fulfill the physics mission of the experiment.

II. POLOIDAL FLUX BALANCE EQUATION

To introduce these empirical models, we first derive an equation for the time variation of the magnetic flux in the plasma-poloidal field (PF) coil system. We proceed heuristically, making use of the following considerations:

1. The flux balance satisfies the following equation:

$$\Delta\Psi_c = \Delta\Psi_p \ , \tag{1}$$

where

$\Delta\Psi_c$ = fraction of the flux variation produced by the PF coils that is used to drive the plasma current

$\Delta\Psi_p$ = total plasma flux consumption.

2. The terms $\Delta\Psi_c$ and $\Delta\Psi_p$ can be divided, as a function of the radial coordinate R, into terms internal to the plasma for $R_b \le R \le R_a$ (where $R_b = R_0 - a$ is the radial coordinate of the plasma boundary, R_0 and a are the major and minor radii of the plasma cross section, respectively, and $R = R_a$ is the coordinate of the plasma magnetic axis) and terms external to the plasma for $0 \le R \le R_b$. Therefore, we can write

$$\Delta\Psi_c(R_a) = \Delta\Psi_{c,int}(R_a) + \Delta\Psi_{c,ext} \tag{2}$$

and

$$\Delta\Psi_p(R_a) = \Delta\Psi_{int}(R_a) + \Delta\Psi_{ext} \ , \tag{3}$$

where it has been specified that the internal and total values of the poloidal flux are evaluated up to the location of the magnetic axis (the external component is clearly evaluated at the plasma boundary). Before substituting Eqs. (2) and (3) into Eq. (1), it is opportune to specify how the different terms are defined and calculated.

3. Inside the plasma, we can write

$$\Delta\Psi_{int}(R_a) = \Delta\Psi_{ind} + \Delta\Psi_{res} \ , \tag{4}$$

where

$\Delta\Psi_{ind}$ = internal inductive flux consumption

$\Delta\Psi_{res}$ = internal resistive flux consumption.

To evaluate the internal inductive flux consumption, it is possible to proceed in two different ways. This gives rise to two different formulations of the flux balance equation, Eq. (1).

4. The term $\Delta\Psi_{ind}$ can be evaluated by using only the poloidal magnetic field produced by the plasma current ($\Delta\Psi_{ind,p}$, where the subscript p refers to the plasma poloidal magnetic field). In doing so, it becomes natural to write the flux balance equation by assuming the magnetic axis as the reference point. Thus, Eq. (1) can be rewritten as

$$\Delta\Psi_{c,int}(R_a) + \Delta\Psi_{c,ext} = \Delta\Psi_{res} + \Delta\Psi_{ind,p} + \Delta\Psi_{ext} \ . \tag{5}$$

5. Instead, if the inductive component is evaluated by using the total poloidal magnetic field required by the plasma equilibrium ($\Delta\Psi_{ind}$, where the total magnetic field is given by the superimposition of the field produced by the plasma current and the poloidal field produced by the external field coils), the internal contribution from the PF coils [$\Delta\Psi_{c,int}(R_a)$] is already taken into account [$\Delta\Psi_{ind} = \Delta\Psi_{ind,p} - \Delta\Psi_{c,int}(R_a)$]. In this situation, by using the total poloidal magnetic field, it is reasonable to write a flux balance equation at the plasma boundary, where the flux still internally needed by the plasma ($\Delta\Psi_{res} + \Delta\Psi_{ind}$) must be equal to the flux available at the plasma boundary ($\Delta\Psi_{c,ext} - \Delta\Psi_{ext}$):

$$\Delta\Psi_{c,ext} - \Delta\Psi_{ext} = \Delta\Psi_{res} + \Delta\Psi_{ind} \tag{6}$$

and, therefore, to rewrite Eq. (1) as

$$\Delta\Psi_{c,ext} = \Delta\Psi_{res} + \Delta\Psi_{ind} + \Delta\Psi_{ext} \ . \tag{7}$$

In this paper, we use B_θ as the standard total poloidal magnetic field because it is easier to compare with experimental data and numerical results. Therefore, we use the flux balance at the plasma boundary, given by Eq. (7).

6. Before proceeding, it is worthwhile to specify some of the terms used in the left side of Eq. (6). In particular, as far as the external poloidal flux consumption and production are concerned, the plasma-PF coil system can be reduced in a simplified way to three electrical circuits reproducing the effects of the plasma (with external inductance L_{ext} and toroidal current I_ϕ), the transformer coils (with flux Ψ_{trans}), and the vertical field coils (with flux Ψ_{vert}). The flux $\Psi_{trans}(R)$ in this ideal model is produced by coils that give zero vertical field in the plasma region and is therefore nearly uniform over the entire region outside the transformer coils

$[\Psi_{trans}(R) \equiv \Psi_{trans}(R_b)$ for $R_b \le R \le R_a]$. Its value is limited only by engineering constraints and does not depend on the plasma configuration. Instead, $\Psi_{vert}(R)$ is associated with the vertical field $B_{vert}(R)$ required for the plasma equilibrium, which, in this simplified model, is assumed to be uniform over the plasma region $[B_{vert}(R) \equiv B_{vert}(R_0) \equiv B_{vert}(R_a)$ for $R_b \le R \le R_a]$. Therefore, we write

$$\Psi_{vert}(R) = \pi R^2 B_{vert}(R_0) \ , \tag{8}$$

and the value of $\Psi_{vert}(R)$ is determined by the particular final plasma equilibrium. The external poloidal flux variation supplied by the coils can be written as

$$\begin{aligned}\Delta\Psi_{c,ext} &= \Delta\Psi_c(R_a) - \Delta\Psi_{c,int}(R_a) \\ &= \Delta(M_{trans}\Psi_{trans}) + \Delta\Psi_{vert}(R_a) \\ &\quad - [\Delta\Psi_{vert}(R_a) - \Delta\Psi_{vert}(R_b)] \\ &= \Delta(M_{trans}\Psi_{trans}) + \Delta\Psi_{vert}(R_b) \\ &= \Delta(M_{trans}\Psi_{trans}) + \Delta[M_{vert}\bar{\Psi}_{vert}(R_0)] \ , \end{aligned} \tag{9}$$

where

M_{trans}, M_{vert} = mutual inductance coefficients between the plasma and the respective external circuits

$\bar{\Psi}_{vert}(R_0)$ = opportune averaged value[10] of the poloidal flux produced by the external coils inside the plasma region.

Following our definition, Ψ_{trans} is uniform over the plasma volume, and the value linked to the plasma boundary is equal to the value on the magnetic axis. Therefore, setting $M_{trans}\Psi_{trans} = \Psi_{trans}(R_b)$, we can rewrite Eq. (9) as

$$\Delta\Psi_{c,ext} = \Delta\Psi_{trans}(R_b) + \Delta[M_{vert}\bar{\Psi}_{vert}(R_0)] \ . \tag{10}$$

The external poloidal flux variation at the plasma boundary, considering what happens outside the plasma, can therefore be written as

$$\begin{aligned}&\Delta\Psi_{c,ext} - \Delta\Psi_{ext} \\ &\quad = \Delta\Psi_{trans}(R_b) + \Delta[M_{vert}\bar{\Psi}_{vert}(R_0)] - \Delta(L_{ext}I_\phi) \ , \end{aligned} \tag{11}$$

where L_{ext} and M_{vert} are functions of the plasma equilibrium alone[10] and do not depend on the relative position between plasma and coils.

7. Rearranging the terms of Eqs. (6) and (11), we can rewrite Eq. (7) as

$$\begin{aligned}&\Delta\Psi_{trans}(R_b) + \Delta[M_{vert}\bar{\Psi}_{vert}(R_0)] \\ &\quad = \Delta\Psi_{ind} + \Delta\Psi_{res} + \Delta(L_{ext}I_\phi) \ , \end{aligned} \tag{12}$$

where the right side represents the total poloidal flux consumed by the plasma, already reduced by the internal contribution from the PF coils, and the left side is the available flux from the coils, which is linked to the plasma column and drives the plasma current.

8. To provide the kind of information usually required by engineers, i.e., the value of the poloidal flux variation in R_0 that the PF system must supply between time $t = 0$ (breakdown) and time t, it is opportune to transform the poloidal flux balance, Eq. (12), at the plasma boundary in the poloidal flux balance equation in R_0, by adding to both sides the flux variation produced by the coils $\Delta\Psi_{c,int}(R_0)$ inside the plasma regions between R_b and R_0:

$$\Delta\Psi_{c,int}(R_0) = \left[1 - M_{vert}\frac{\bar{\Psi}_{vert}(R_0)}{\Psi_{vert}(R_0)}\right]\Psi_{vert}(R_0) \ ; \tag{13}$$

we then obtain

$$\begin{aligned}&\Delta\Psi_{trans}(R_b) + \Delta\Psi_{vert}(R_0) \\ &\quad = \Delta\Psi_{ind} + \Delta\Psi_{res} + \Delta(L_{ext}I_\phi) \\ &\qquad + \left[1 - M_{vert}\frac{\bar{\Psi}_{vert}(R_0)}{\Psi_{vert}(R_0)}\right]\Psi_{vert}(R_0) \ , \end{aligned} \tag{14}$$

where the left side represents the total flux supplied by the coils in R_0

$$\Delta\Psi_c(R_0) = \Delta\Psi_{trans}(R_b) + \Delta\Psi_{vert}(R_0) \ , \tag{15}$$

to link the amount $\Delta\Psi_{c,ext}$ to the plasma column. The value of $\Delta\Psi_c(R_0)$ plus all the contributions from higher order fields may be provided by an MHD and transport code such as the TSC code. The right side of Eq. (14) can be seen as an effective total poloidal flux consumed by the plasma in R_0:

$$\Delta\Psi_p(R_0) = \Delta\Psi_{ind} + \Delta\Psi_{res} + \Delta\Psi_{ext}(R_0) \ , \tag{16}$$

where $\Delta\Psi_{ext}(R_0)$ is given by

$$\begin{aligned}&\Delta\Psi_{ext}(R_0) \\ &\quad = \Delta(L_{ext}I_\phi) + \left[1 - M_{vert}\frac{\bar{\Psi}_{vert}(R_0)}{\Psi_{vert}(R_0)}\right]\Psi_{vert}(R_0) \ . \end{aligned} \tag{17}$$

We define, as shown in Sec. III.B, this effective external inductance evaluated in R_0 as

$$\begin{aligned}&L_{ext}(R_0) \\ &\quad \equiv L_{ext} + \left[1 - M_{vert}\frac{\bar{\Psi}_{vert}(R_0)}{\Psi_{vert}(R_0)}\right]\frac{\Psi_{vert}(R_0)}{I_\phi} \ , \end{aligned} \tag{18}$$

where the last term in the right side of Eq. (18) can be interpreted[11] as an additional term to the external inductance L_{ext}, and, therefore, rewrite Eq. (16) as

$$\Delta\Psi_p(R_0) = \Delta\Psi_{ind} + \Delta\Psi_{res} + \Delta[L_{ext}(R_0)I_\phi] \ . \tag{19}$$

9. Now we add to the effective plasma consumption in Eq. (19) the initial flux variation used during the

breakdown phase of the discharge ($\Delta\Psi_{breakd}$) and the poloidal flux reduction due to the presence of the bootstrap current ($\Delta\Psi_{bs}$):

$$\Delta\Psi_p(R_0) = \Delta\Psi_{ind} + \Delta\Psi_{res} + \Delta[L_{ext}(R_0)I_\phi] + \Delta\Psi_{breakd} - \Delta\Psi_{bs} \ . \quad (20)$$

Note that except for the initial breakdown flux variation, the resistive contribution is proportional to the toroidal plasma current variation $\Delta I_\phi = I_\phi$. Thus, to include the reduction due to the bootstrap current I_{bs}, it is sufficient to define an effective plasma current induced by the PF system as

$$I_{eff} \equiv I_p - I_{bs} \ , \quad (21)$$

and to rewrite Eq. (20) as

$$\Delta\Psi_p(R_0) = \Delta\Psi_{ind}(I_\phi) + \Delta\Psi_{res}(I_{eff}) + \Delta[L_{ext}(R_0)I_\phi] + \Delta\Psi_{breakd} \ . \quad (22)$$

10. In summary, the exact balance equations, at different radial locations, are

at the plasma center R_0:

$$\Delta\Psi_{trans} + \Delta\Psi_{vert}(R_0) = \Delta\Psi_{ind}(I_\phi) + \Delta\Psi_{res}(I_{eff}) + \Delta[L_{ext}(R_0)I_\phi] + \Delta\Psi_{breakd} \ , \quad (23)$$

at the plasma boundary R_b:

$$\Delta\Psi_{trans} + \Delta\Psi_{vert}(R_b) = \Delta\Psi_{ind}(I_\phi) + \Delta\Psi_{res}(I_{eff}) + \Delta[L_{ext}I_\phi] + \Delta\Psi_{breakd} \ , \quad (24)$$

at the magnetic axis R_a:

$$\Delta\Psi_{trans} + \Delta\Psi_{vert}(R_a) = \Delta\Psi_{ind,p}(I_\phi) + \Delta\Psi_{res}(I_{eff}) + \Delta[L_{ext}I_\phi] + \Delta\Psi_{breakd} = \Delta\Psi_{ind}(I_\phi) + \Delta\Psi_{res}(I_{eff}) + \Delta[L_{ext}(R_a)I_\phi] + \Delta\Psi_{breakd} \ , \quad (25)$$

where $L_{ext}(R_a)$ is defined, following the same procedure used for $L_{ext}(R_0)$, as

$$L_{ext}(R_a) \equiv L_{ext} + \left[1 - M_{vert}\frac{\bar{\Psi}_{vert}(R_0)}{\Psi_{vert}(R_a)}\right]\frac{\Psi_{vert}(R_a)}{I_\phi} \ . \quad (26)$$

In the rest of the paper, we refer to the balance equation at the plasma center given by Eq. (23).

The internal flux consumption $[\Delta\Psi_{ind}(I_\phi) + \Delta\Psi_{res}(I_{eff})]$ is the most difficult term to evaluate. In the following sections, we discuss two different methods[12,13] and present analytical and numerical results obtained for Ignitor.

III. HEURISTIC MODELS

III.A. Internal Flux Requirement

The internal flux used to drive a certain plasma current has been divided into two parts: inductive (nondissipative) and resistive. The two methods that are examined, briefly reiterating the exposition presented in Ref. 14, give different ratios of the dissipative part of the internal flux consumption with respect to the nondissipative part, although the overall internal flux requirement should be the same.

III.A.1. Poynting Method

Starting from Faraday's and Ampere's laws,[12,14]

$$-\frac{\partial \boldsymbol{B}}{\partial t} = \nabla \times \boldsymbol{E} \quad (27)$$

and

$$\mu_0 \boldsymbol{J} = \nabla \times \boldsymbol{B} \ , \quad (28)$$

and taking the scalar product of Eq. (27) with $\boldsymbol{B}_\theta$ and Eq. (28) with $\boldsymbol{E}_\phi$ (where ϕ and θ indicate the toroidal and poloidal directions, respectively) and subtracting the two equations, we obtain

$$-\frac{\partial \boldsymbol{B}_\theta^2}{\partial t} - 2\mu_0 \boldsymbol{E}_\phi \cdot \boldsymbol{J}_\phi = 2\nabla \cdot (\boldsymbol{E}_\phi \times \boldsymbol{B}_\theta) \ . \quad (29)$$

The integration of Poynting's theorem, given by Eq. (29), over the plasma volume gives the poloidal magnetic energy balance[14]:

$$-\int_V \frac{1}{2\mu_0}\frac{\partial \boldsymbol{B}_\theta^2}{\partial t}\, dV - \int_V \boldsymbol{E}_\phi \cdot \boldsymbol{J}_\phi \, dV = -V_\phi(R_b,t)I_\phi(t) \ . \quad (30)$$

Now solving Eq. (30) with respect to the toroidal loop voltage $V_\phi(R_b,t)$, neglecting a term due to change in the geometry, and integrating over time, we obtain the Poynting energy form of the poloidal flux balance:

$$\Delta\Psi_{int}^P \equiv \int V_\phi(R_b,t)\, dt \simeq \int \frac{dt}{I_\phi(t)}\left[\frac{\partial W_{B_\theta}(t)}{\partial t} + \int_V \boldsymbol{E}_\phi \cdot \boldsymbol{J}_\phi \, dV\right] \ , \quad (31)$$

where

$\Delta\Psi_{int}^P$ = total internal flux variation (the superscript P refers to Poynting method)

$$W_{B_\theta}(t) = \int_V \frac{B_\theta^2}{2\mu_0}\, dV$$

= poloidal magnetic energy content of the plasma.

Now defining an internal inductance

$$L_{int}^{P} \equiv \frac{\mu_0 R_0 l_i(t)}{2} = \frac{2W_{B_\theta}(t)}{I_\phi^2(t)} , \quad (32)$$

where the Shafranov inductance $l_i(t)$ is given by

$$l_i(t) \equiv \frac{4W_{B_\theta}(t)}{\mu_0 R_0 I_\phi^2(t)} , \quad (33)$$

and defining an effective resistivity

$$R_{eff} \equiv \frac{1}{I_\phi^2(t)} \int_V \boldsymbol{E}_\phi \cdot \boldsymbol{J}_\phi \, dV , \quad (34)$$

we can rewrite Eq. (31) as

$$\Delta\Psi_{int}^{P} = \Delta[L_{int}^{P} I_\phi(t)] - \int \frac{1}{2} I_\phi(t) \frac{\partial L_{int}^{P}(t)}{\partial t} \, dt + \int I_\phi(t) R_{eff}(t) \, dt , \quad (35)$$

where the second term on the right side of Eq. (35), which was originally[12] defined as part of the inductive flux, depends on the plasma evolution. Instead, following the notation[15] originally attributed to Sugihara, we can define the effective internal inductive flux variation linked to the external circuits as[14,15]

$$\Delta\Psi_{ind}^{P}(t) \equiv \Delta[L_{int}^{P}(t) I_\phi(t)] \quad (36)$$

and the flux dissipated to establish the poloidal magnetic energy content of the plasma as

$$\Delta\Psi_{res}^{P} = \int \left[-\frac{1}{2} I_\phi(t) \frac{\partial L_{int}^{P}(t)}{\partial t} + I_\phi(t) R_{eff}(t) \right] dt . \quad (37)$$

Therefore, we can rewrite the internal poloidal flux balance as

$$\Delta\Psi_{int}^{P} = \Delta\Psi_{ind}^{P} + \Delta\Psi_{res}^{P} . \quad (38)$$

In this way, as reported in Ref. 16, the internal inductive flux $\Delta\Psi_{ind}^{P}$ becomes a property of any equilibrium and can be evaluated by time-independent equilibrium calculation. The internal resistive flux $\Delta\Psi_{res}^{P}$, which includes the dissipation associated with plasma current penetration process, requires a time-dependent simulation of the current profile evolution.

III.A.2. Faraday Method

In this approach,[13,14] the magnetic flux balance is derived by integrating Faraday's law [see Eq. (27)] over a toroidal strip S_θ bounded by the magnetic axis ($R = R_a$) and the plasma edge ($R = R_b$):

$$-\int_{S_\theta} \frac{\partial \boldsymbol{B}}{\partial t} \cdot d\boldsymbol{S}_\theta = \int_{S_\theta} (\nabla \times \boldsymbol{E}) \cdot d\boldsymbol{S}_\theta = \oint_{R_a} \boldsymbol{E} \cdot d\boldsymbol{l}_\phi - \oint_{R_b} \boldsymbol{E} \cdot d\boldsymbol{l}_\phi = V_\phi(R_a,t) - V_\phi(R_b,t) . \quad (39)$$

Now, defining the inductive component $\Delta\Psi_{ind}^{F}$ as

$$\Psi_{ind}^{F} \equiv \int_{S_\theta} \boldsymbol{B}_\theta \cdot d\boldsymbol{S}_\theta , \quad (40)$$

solving Eq. (39) with respect to $V_\phi(R_b,t)$, neglecting a term due to change in geometry, and integrating over time, we obtain the poloidal flux equation:

$$\Delta\Psi_{int}^{F}(t) \equiv \int V_\phi(R_b,t) \, dt \simeq \int \left[V_\phi(R_a,t) + \frac{\partial \Psi_{ind}^{F}}{\partial t} \right] dt . \quad (41)$$

By defining an internal inductance

$$L_{int}^{F} \equiv \frac{\mu_0 R_0 h_i(t)}{2} = \frac{\Psi_{ind}^{F}}{I_\phi} , \quad (42)$$

where the flux inductance $h_i(t)$ is given by

$$h_i(t) \equiv \frac{2\Psi_{ind}^{F}}{\mu_0 R_0 I_\phi} , \quad (43)$$

we can rewrite the magnetic flux balance equation as

$$\Delta\Psi_{int}^{F}(t) = \Delta[L_{int}^{F}(t) I_\phi(t)] + \int V_\phi(R_a,t) \, dt . \quad (44)$$

Note that the flux inductance h_i is different from the Shafranov inductance l_i used in the Poynting method, which was defined by the magnetic energy content of the plasma. The first term in Eq. (44), representing the internal inductive flux variation, depends only on the particular plasma equilibrium and can be calculated using a time-independent equilibrium code. The last term can be rewritten as

$$\int V_\phi(R_a,t) \, dt = 2\pi R_a \int \frac{J_\phi(R_a,t)}{\sigma(R_a,t)} \, dt , \quad (45)$$

and it represents the resistive loss on the axis [$\sigma(R_a,t)$ is the plasma conductivity and $J_\phi(R_a,t)$ is the toroidal plasma current density on the axis]. As with any other dissipative term, it must be evaluated from a time-dependent simulation.

III.B. External Flux Requirement

The effective external plasma flux variation evaluated at the plasma center is given, as shown in Sec. I, by

$$\Delta\Psi_{ext}(R_0) = \Delta[L_{ext}(R_0) I_\phi] = \Delta[L_{ext} I_\phi] + \left[1 - M_{vert} \frac{\bar{\Psi}_{vert}(R_0)}{\Psi_{vert}(R_0)} \right] \times \Psi_{vert}(R_0) , \quad (46)$$

where the plasma self-inductance L_{ext} and the mutual inductance M_{vert} depend only on the geometric characteristics of the last closed flux surface. The value of

M_{vert} can be calculated if a reference value for the average flux $\bar{\Psi}_{vert}(R_0)$ produced by the vertical coils is specified. Assuming, as has been done in Ref. 10, that

$$\bar{\Psi}_{vert}(R_0) = \pi R_0^2 B_{vert}(R_0) \ , \tag{47}$$

where $B_{vert}(R_0)$ is the vertical equilibrium field, the last term in Eq. (46) can be simplified and rewritten as[11]

$$\left[1 - M_{vert}\frac{\bar{\Psi}_{vert}(R_0)}{\Psi_{vert}(R_0)}\right]\Psi_{vert}(R_0) = (1 - M_{vert})\pi R_0^2 B_{vert}(R_0) \ , \tag{48}$$

and using the Shafranov formula for $B_{vert}(R_0)$,

$$B_{vert}(R_0) = \frac{\mu_0 I_\phi}{4\pi R_0}\left[\ln\left(\frac{8R_0}{a\kappa^{1/2}}\right) + \beta_p + \frac{l_i - 3}{2}\right] \ , \tag{49}$$

where

a = plasma minor radius

κ = elongation of the plasma cross section

β_p = plasma poloidal beta,

we obtain the following expression for the effective external inductance evaluated in R_0:

$$L_{ext}(R_0) = L_{ext} + \frac{\mu_0 R_0}{4}(1 - M_{vert}) \times \left[\ln\left(\frac{8R_0}{a\kappa^{1/2}}\right) + \beta_p + \frac{l_i - 3}{2}\right] \ . \tag{50}$$

For a circular plasma with a large aspect ratio, we have $M_{vert} = 1$ and

$$L_{ext} = \mu_0 R_0[\ln(8R_0/a) - 2] \ , \tag{51}$$

while for a toroidal configuration with an inverse aspect ratio $\epsilon = a/R_0$ and an elliptical cross section with elongation κ, L_{ext} and M_{vert} must be evaluated numerically. Useful analytical formulas for L_{ext} and M_{vert} were obtained in Ref. 10 for an elliptical cross section by fitting numerical results:

$$L_{ext} \simeq \mu_0 R_0[f_1(\epsilon)(1 - \epsilon)]/[1 - \epsilon + f_2(\epsilon)\kappa] \tag{52}$$

and

$$M_{vert} \simeq [(1 - \epsilon)^2]/[(1 - \epsilon)^2 f_3(\epsilon) + f_4(\epsilon)\kappa^{1/2}] \ , \tag{53}$$

where

$$f_1(\epsilon) \simeq (1 + 1.81\epsilon^{1/2} + 2.05\epsilon)\ln(8/\epsilon) - (2 + 9.25\epsilon^{1/2} - 1.21\epsilon) \ ,$$

$$f_2(\epsilon) \simeq 0.73\epsilon^{1/2}(1 + 2\epsilon^4 - 6\epsilon^5 + 3.7\epsilon^6) \ ,$$

$$f_3(\epsilon) \simeq 1 + 0.98\epsilon^2 + 0.49\epsilon^4 + 1.47\epsilon^6 \ ,$$

and

$$f_4(\epsilon) \simeq 0.25\epsilon(1 + 0.84\epsilon - 1.44\epsilon^2) \ . \tag{54}$$

IV. APPLICATION TO THE IGNITOR CONFIGURATION

IV.A. Plasma Scenarios

The basic reference plasma dimensions and parameters of Ignitor[17] (see Fig. 1) are reported in Table I.

To design a PF system able to meet the requirements of different plasma performances and parameters, several plasma scenarios have been analyzed by means of the TSC modeling code, to discover which one presents the greatest demands. In particular, we present the results relative to seven different plasma scenarios where a maximum plasma current I_ϕ of 8, 10, or 12 MA is induced by using different durations of the current ramp phase, different values of the injected power, and different locations of the magnetic null point at the breakdown (close to the inside or the outside limiter). The main parameters of these scenarios and the corresponding plasma performances, relative to the time t when the maximum plasma temperature (cases 1 through 4) or when ignition is reached (cases 5 through 7), are reported in Table II. Here, the performance parameter Q is defined under transient conditions as $Q \equiv (5P_\alpha)/(P_{oh} + P_{inj} - \dot{W})$, where $\dot{W}$ is the rate of change of the internal energy. Figure 2 reports typical poloidal magnetic flux contours (case 7, Table II) for a plasma at the start of the TSC calculation and at the beginning of the flattop. The final contours are similar for all cases. The transport models used in these simulations, as well as all the other input parameters, are the same as in Ref. 6. We write the total electron thermal diffusion coefficient as

$$\chi_e = \chi_e^{oh} + \chi_e^{non\text{-}oh} \ , \tag{55}$$

where χ_e^{oh} is an extension[5,6] of the Coppi-Mazzucato-Grüber[18,19] diffusion coefficient to regimes in which ohmic heating is no longer dominant, and $\chi_e^{non\text{-}oh}$ is an anomalous electron heat diffusion coefficient arising when non-ohmic heating is present.[5,6] In particular, $\chi_e^{non\text{-}oh}$ is given by

$$\chi_e^{non\text{-}oh} = \left(\frac{P_{heat} - P_{oh}}{P_{heat}}\right) C^{aux}\chi_e^{aux} \ , \tag{56}$$

where

P_{heat} = total input power ($P_{heat} = P_{oh} + P_\alpha + P_{inj}$, where P_{oh} is the ohmic heating power, P_α is the alpha-particle heating power, and P_{inj} is the injected heating power)

C^{aux} = numerical coefficient

χ_e^{aux} = anomalous electron heat diffusion coefficient due to the combined excitation of the "ubiquitous" trapped electron mode[20,21] and the collisional impurity-driven mode.[22]

The numerical coefficient C^{aux} is evaluated in such a way that the total energy confinement time τ_E reproduces present-day experiments with injected heating in

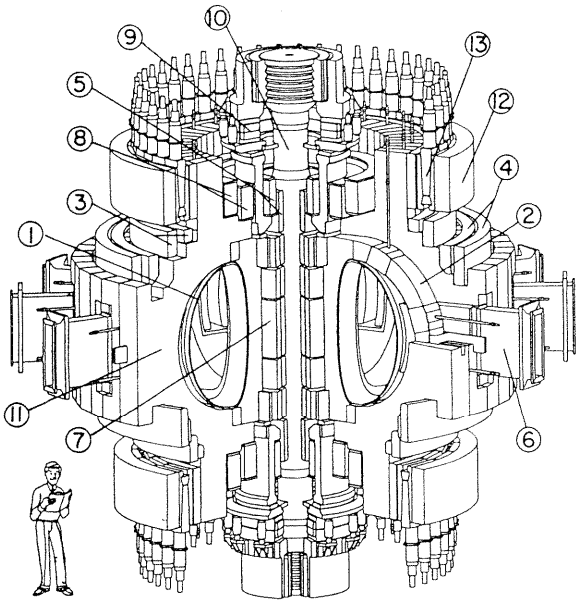

① PLASMA CHAMBER
② TOROIDAL MAGNET
③ SHAPING COILS
④ EQUILIBRIUM COILS
⑤ OUTER TRANSFORMER COIL
⑥ EQUATORIAL PORTS
⑦ CENTRAL SOLENOID
⑧ SHAPING AND TRANSFORMER COIL
⑨ AXIAL PRESS
⑩ CENTRAL POST
⑪ C-CLAMP
⑫ BRACING RING
⑬ TENSIONING WEDGES
R_0 = 1320 mm
a = 470 mm
b = 870 mm

Fig. 1. Axonometric view of the Ignitor machine. The plasma column has R_0 (major radius) $\simeq 1.32$ m, $a \times b$ (minor radii) $\simeq 0.47 \times 0.87$ m^2, and δ_G (triangularity) $\simeq 0.4$. The toroidal plasma current is $I_p \lesssim 12$ MA, and the toroidal field on axis is $B_\phi \lesssim 13$ T, with a further contribution from paramagnetic effect [$\Delta B_\phi \simeq 1.5$ T for a poloidal (paramagnetic) current $I_\theta \lesssim 10$ MA].

the so-called L mode. The ion thermal diffusion coefficient is written as[5,6]

$$\chi_i = \chi_i^{neo} + \gamma_i \chi_e^{non\text{-}oh} \quad , \tag{57}$$

where

χ_i^{neo} = collisional (so-called neoclassical) diffusion coefficient[23]

γ_i = numerical coefficient typically in the range between 0 and 2 ($\gamma_i = 0.5$ in the simulations reported here).

In cases 5, 6, and 7, all the data and the evaluation of the poloidal flux requirement refer to the time when ignition is achieved. This is justified because transport simulations[5,6,17] have shown that after ignition is reached, the maximum value of I_ϕ is not necessary to sustain the ignited state since the fusion alpha-particle power takes care of the power balance. Moreover, during the rampdown of the plasma current, as has been shown experimentally in the Tokamak Fusion Test Reactor [24] (TFTR) and confirmed by transport simulations,[17] the current density is reduced only in the external plasma region ($r \geq \frac{2}{3}a$), and thus, the confinement properties of the discharge do not deteriorate with respect to the full plasma current case. Thus, if this operational procedure is adopted, the poloidal flux requirement reaches a maximum at ignition and decreases afterward.

TABLE I

Reference Design Parameters of the Ignitor Configuration

Major radius of the plasma column	$R_0 \simeq 1.32$ m
Minor radius of the plasma cross section	$a \simeq 0.47$ m
Triangularity of the plasma cross section	$\delta_G \simeq 0.4$
Elongation of the plasma cross section	$\kappa \simeq 1.85$
Plasma current in the toroidal direction	$I_\phi \lesssim 12$ MA
Vacuum toroidal magnetic field at R_0	$B_\phi \lesssim 13$ T
Safety factor at the plasma edge	$q_\Psi(a) \lesssim 3.5$
Injected heating power (ion cyclotron resonance heating at $f \simeq 130$ MHz)	$P_{inj} \lesssim 18$ MW

The values (evaluated from the TSC simulations) at the start (SOFT) and end of the flattop or at ignition (EOFT) of the Shafranov inductance l_i, the flux inductance h_i, the poloidal beta β_p, the bootstrap current I_{bs}, and the time-averaged value of the toroidal loop voltage on the magnetic axis $\bar{V}_\phi(R_a)$ during the flattop are reported in Table III for the seven plasma scenarios described.

Note that the values of the internal inductance at the SOFT are lower than those at the EOFT. This means, because of the relatively short current ramp compared with the diffusion resistive time scale and the relatively high value of plasma current, the current profile at the SOFT has not yet reached the steady-state, fully penetrated profile (see Fig. 3). This feature is useful[5,6] to control the size of the region where the magnetic field

TABLE II

Different Plasma Scenarios for the Ignitor Configuration

	Case						
	1	2	3	4	5	6	7
Plasma current, I_ϕ (MA)	8	8	10	10	10	12	12
Location of the null	Out	Out	Out	Out	Out	Out	In
Numerical coefficient, C^{aux}	1.0	1.0	1.0	1.0	0.66	1.0	1.0
Injected heating power, P_{inj} (MW)	0	10	0	10	0	0	0
Toroidal field at R_0, B_ϕ (T)	10	10	11	11	11	13	13
Poloidal field, B_θ (T)	2.7	2.7	3.3	3.3	3.3	3.9	3.9
Vertical field at R_0, B_{vert} (T)	1.2	1.2	1.5	1.5	1.5	1.8	1.8
Rampup time for I_ϕ, t_r (s)	3.0	3.0	3.5	3.5	3.5	4.0	3.0
Time, t (s)	9.0	9.0	8.5	8.5	5.5	5.0	4.3
Peak electron density, n_{e0} (10^{20} m^{-3})	8.0	8.0	9.0	9.0	9.0	10.5	10.5
Peak temperature, T_0 (keV)	6.4	11.4	9.7	17.2	13.2	11.8	11.0
Energy confinement time, τ_E (s)	0.71	0.35	0.53	0.28	0.57	0.59	0.66
Alpha-particle power, P_α (MW)	2.3	10.3	10.8	38.0	20.0	21.0	17.8
Ohmic power, P_{oh} (MW)	6.1	4.0	7.1	4.0	5.8	8.9	9.5
Effective charge, Z_{eff}	1.2	1.2	1.2	1.2	1.2	1.2	1.2
Performance parameter, Q	2.0	4.0	8.0	14.0	∞	∞	∞

line parameter q is less than or equal to 1, and to avoid the excitation of sawtooth oscillations. It also means that a significant amount of poloidal flux must be provided during the flattop to compensate not only for the resistive loss, but also for the increase in the magnetic energy content of the plasma. Furthermore, the slow inward diffusion of the plasma current compared to the growth of the central temperature generates an inhomogeneous toroidal loop voltage (see Fig. 4) that is peaked near the plasma edge and allows a large value of ohmic heating[4-6] at a high central temperature, as shown in Table II.

The values of h_i reported in Table III, which were obtained from a TSC simulation, have been checked against the values obtained by means of equilibrium calculations carried out with the TEQ code and with the following experimental relationships[16] that correlate the value of h_i to the value of l_i:

$$h_i \simeq \begin{cases} 1.01 \times l_i + 0.48 & \text{for } l_i \geq 0.75 \quad (58) \\ 1.45 \times l_i + 0.15 & \text{for } l_i \leq 0.75 \; . \quad (59) \end{cases}$$

As shown in Table IV, for a particular plasma scenario (case 6, Table II), the three different evaluations

TABLE III

TSC Evaluation of l_i, h_i, I_{bs}, and $\bar{V}_\phi(R_a)$ for Different Plasma Scenarios

	Case						
	1	2	3	4	5	6	7
l_i (SOFT)	0.68	0.68	0.68	0.68	0.68	0.68	0.64
l_i (EOFT)	1.04	1.04	1.0	1.0	0.86	0.78	0.76
h_i (SOFT)	1.14	1.14	1.14	1.14	1.14	1.14	1.08
h_i (EOFT)	1.53	1.53	1.49	1.49	1.35	1.27	1.25
β_p (SOFT)	0.11	0.15	0.10	0.13	0.10	0.09	0.09
β_p (EOFT)	0.14	0.20	0.15	0.23	0.15	0.15	0.13
I_{bs} (SOFT) (MA)	0.48	0.7	0.55	0.8	0.55	0.6	0.6
I_{bs} (EOFT) (MA)	0.52	0.9	0.7	1.0	0.95	1.1	1.0
$\bar{V}_\phi(R_a)$ (V)	0.42	0.18	0.38	0.15	0.32	0.3	0.3

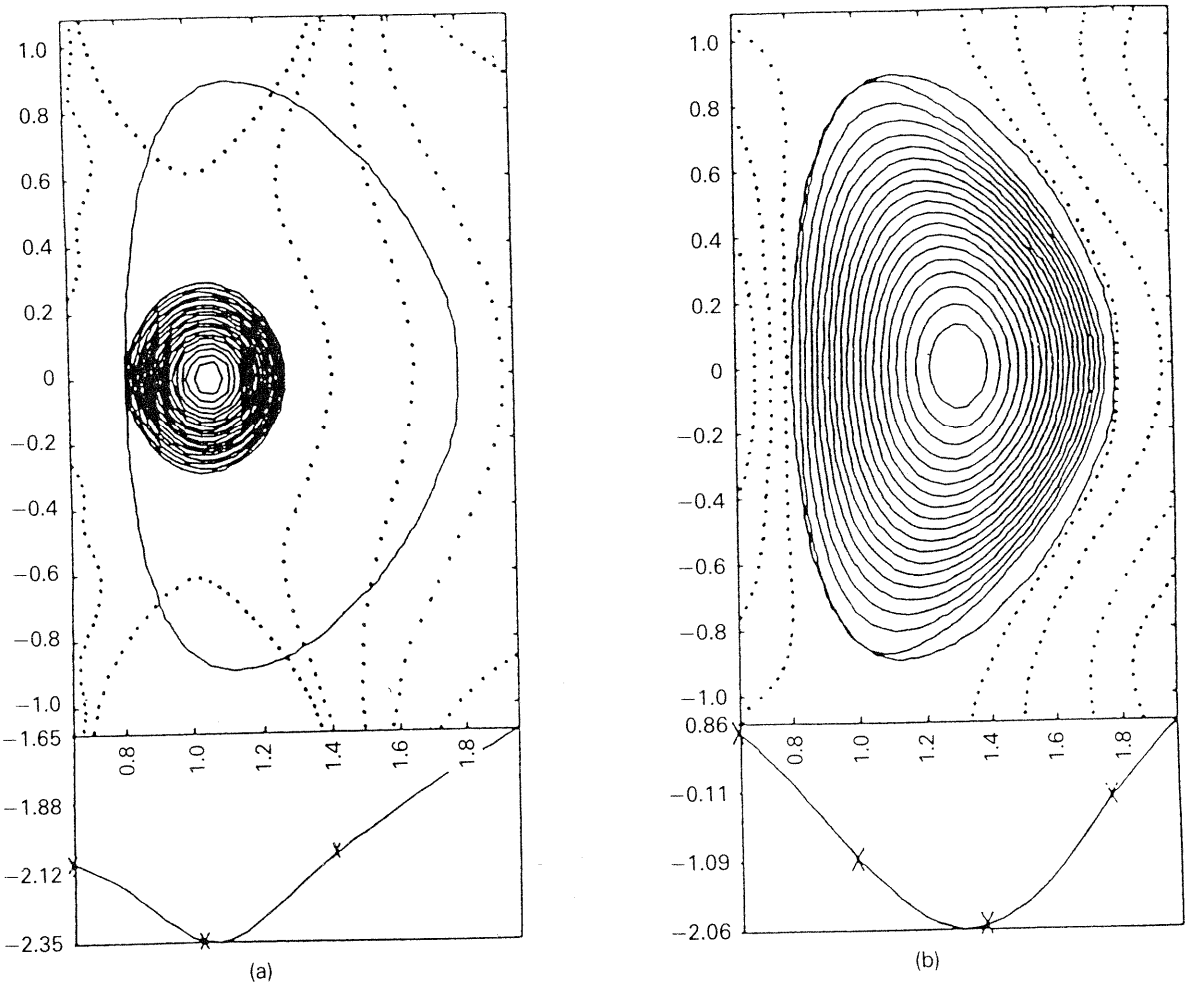

Fig. 2. Typical poloidal magnetic flux contours for a plasma starting on the inside limiter (case 7, Table II): (a) at the start of calculation and (b) at SOFT. The lower plots show the normalized poloidal flux on the horizontal midplane (in Wb/2π). The final current is $I_\phi \simeq 12$ MA, and $B_\phi \simeq 13$ T. The final contours are similar for all the cases.

of h_i, for the same value of l_i, differ by only a few percent.

These results show that the internal inductive flux consumption can be evaluated correctly by using an equilibrium code or, at least for this Ignitor configuration, by means of a simple experimental scaling with l_i, such as the one derived by the Joint European Torus (JET) Team.[16]

IV.B. Estimates of the Poloidal Flux Requirement

All seven discharges produce at SOFT, and maintain throughout the flattop, the plasma configuration that is described in Table I. Therefore, the external inductance L_{ext} and the mutual vertical inductance M_{vert}, which are functions of geometrical parameter only, will be the same in all the discharges [from Eqs. (51) through (54), we obtain $L_{ext} \simeq 1.21$ (μH) and $M_{vert} \simeq 0.68$]. Furthermore, the additional term contained in $L_{ext}(R_0)$, which is a function of l_i and β_p, does not change significantly, as shown in Table V. In this table, the values of $L_{ext}(R_0)$ at SOFT and at EOFT, evaluated using Eqs. (51) through (54) and the Ignitor parameters

TABLE IV

Comparison Between Values of h_i Derived from Experimental Relationships and TSC and TEQ Simulations for Case 6

Method	Experimental Relationships	TSC	TEQ
l_i (SOFT)	0.68	0.68	0.68
h_i (SOFT)	1.14	1.16	1.17
l_i (EOFT)	0.78	0.78	0.78
h_i (EOFT)	1.27	1.29	1.31

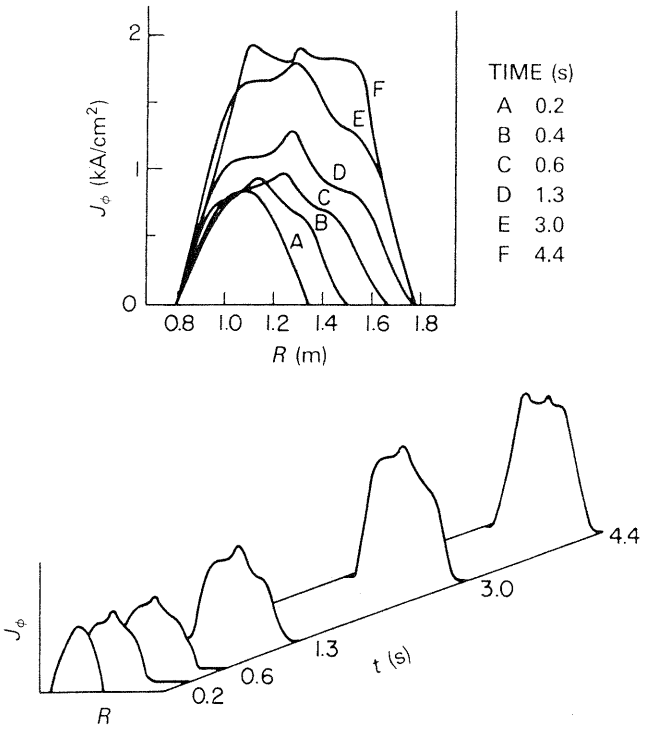

Fig. 3. Time evolution of the toroidal plasma current density profile as a function of the plasma radius, for case 7 of Table II.

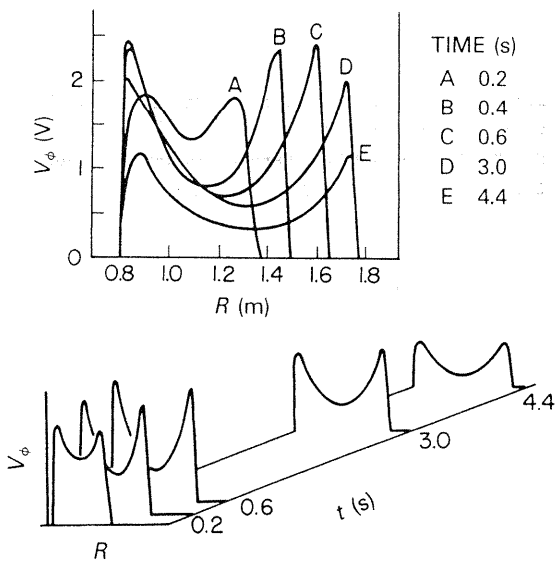

Fig. 4. Time evolution of the toroidal loop voltage as a function of the plasma radius, for case 7 of Table II.

reported in Tables I, II, and III, are compared with the values obtained by means of TSC and TEQ simulations. Note that the value of the external inductance given by the TEQ is the value $L_{ext}(R_a)$ [see Eq. (26)],

TABLE V

Comparison Between Values of $L_{ext}(R_0)$ Derived from Analytical Formulas and TSC and TEQ Simulations for Case 6

Method	Analytical Formulas	TSC	TEQ
$L_{ext}(R_0)$ (SOFT)	1.44	1.42	1.42
$L_{ext}(R_0)$ (EOFT)	1.46	1.44	1.44

evaluated at the magnetic axis, as is the value given by any other equilibrium code, and must therefore be corrected before being compared with the other estimates.

Thus, to find out which discharge of two with the same plasma current requires a larger poloidal flux, it is sufficient to compare the internal flux requirements. Looking at Tables II and III, we can see that the two auxiliary heated discharges (cases 2 and 4) should present lower poloidal flux requirements than the corresponding ohmic discharges (cases 1 and 3) because of a reduction in the resistive consumption. In particular, this reduction, evaluated to be ~2 V·s by TSC simulations, is due to two phenomena occurring in the auxiliary heated discharges:

1. an increase in the bootstrap current and thus a reduction in the effective plasma current I_{eff} induced by the PF system [see Eq. (21)]
2. an increase in the plasma temperature and thus a reduction in the plasma resistivity, as shown by the values of $\bar{V}_\phi(R_a)$ in Table III.

The 10-MA discharge that reaches ignition (case 5) clearly requires a lower poloidal flux swing than the one that does not reach ignition (case 3), because of a reduction of all the internal terms. A comparison of cases 3 and 5 is useful to underline the relatively high degree of uncertainty in the prediction of the plasma performances. A small reduction in the non-ohmic component (see C^{aux} in Table II) of the thermal diffusion coefficient[6] is sufficient to allow the 10-MA discharge (see case 5, Table II) to reach ohmic ignition with an energy confinement time that is still comparable with the prediction of L-mode scalings.

As far as cases 6 and 7 are concerned, it can be inferred that case 6 will require a larger poloidal flux variation (evaluated to be ~1 V·s by TSC simulation) because it takes a longer time to reach ignition (5.0 s compared with 4.3 s) and thus requires larger resistive consumption, and also because it presents a larger value of the internal inductance (larger magnetic energy content in the plasma and thus larger inductive requirement).

Therefore, to evaluate the maximum poloidal flux variation that must be produced by the transformer, we

concentrate our analysis on cases 1, 3, and 6. In particular, we estimate the poloidal flux requirement by using heuristic models, developed in the framework of the International Thermonuclear Experimental Reactor (ITER) activity[15,16] on a large tokamak data base.

These heuristic models,[15,16] based on the Poynting and Faraday approaches, give the following expression for the dissipative component (including the flux variation used for the breakdown) of the poloidal flux requirement:

$$\Delta\Psi_{res} + \Delta\Psi_{breakd} \simeq (C_{Ejima}\mu_0 R_0) I_{eff} \ (\mathrm{V\cdot s}) \ , \quad (60)$$

where the suggested values[16] for the Ejima coefficient are $C_{Ejima} = 0.4$ for the Poynting approach and $C_{Ejima} = 0.16$ for the Faraday approach. Note[15,16] that the Ejima coefficient has been chosen so as to fit empirical data coming from different machines. As pointed out in the original paper by Ejima et al.,[25] there was considerable scatter of the data about the line of best fit, attributable to differences in the way the discharges were programmed through the current rise.

In Table VI, the evaluations of the poloidal flux requirement at the SOFT given by the two heuristic models are compared using the data reported in Tables I through IV. In particular, as far as the resistive components are concerned, the heuristic expression containing the Ejima coefficient was used to determine the values at SOFT, as suggested in the literature.[15,16,25]

In comparing the results obtained by using the two methods, note the good agreement on the value of the total internal flux consumption $\Delta\Psi_{int}$, which confirms that the relationship between the Ejima coefficient for the two methods suggested by the ITER Team is consistent with the relationship of h_i to l_i, reported by the JET group in Ref. 16. As expected, the Poynting approach predicts a smaller inductive poloidal flux consumption and thus a larger dissipative part of the magnetic flux requirement. The large dissipative component in the Poynting method may be misleading[16] since "a little of this could be saved without reducing current penetration and thereby risking instability." The only resistive consumption that can be reduced, by using noninductive current drive, is the resistive loss on axis.

Taking into account the good agreement between the Faraday and the Poynting methods, from now on we use only the results of the Faraday approach for a rapid comparison with the results obtained with the TSC code (which presents its results according to the Faraday method). The TSC code[7] follows the plasma evolution from the beginning of the current ramp and takes into account the reduction due to the bootstrap current and the exact plasma shape.[4-6] Table VII shows that the TSC results are in good agreement with the estimates derived from the heuristic model. The values at EOFT have been estimated, in the heuristic model based on the Faraday approach, by adding to the value at the SOFT the resistive consumption on axis during the flattop. This last value may be approximated as $\bar{V}_\phi(R_a) \times \Delta t_{flattop}$, where the value of $\bar{V}_\phi(R_a)$ was derived from TSC simulations (see Table III) and $\Delta t_{flattop}$ is the duration of the flattop phase of the discharge.

The estimates differ in the external inductive flux variations. This is mainly due to minor variations of the plasma parameters obtained in the TSC simulations compared with the reference parameters reported in Table I. Furthermore, the analytical estimates are evaluated for an elliptic configuration and do not take into account the significant triangularity of the Ignitor plasma cross section. Therefore, a second-order variations should be expected.

The differences in the evaluation of the internal inductive terms clearly reflect the variations found (see Table IV) in the estimations of h_i. The other discrepancy is found in the resistive components, confirming the relatively high degree of uncertainty in the value of the Ejima coefficient. In fact, the resistive flux consumption strongly depends on the characteristics of the plasma current penetration phase. Numerical TSC simulations (see Table VIII) have shown that by programming the plasma density evolution, it is possible to reduce the dissipative consumption by ~ 0.7 V·s in the three reference cases. This is accomplished by slowly increasing the plasma density during the first part of the current ramp in order to reach a relatively high peak plasma temperature ($T_0 \gtrsim 4$ keV), and thus a low plasma resistivity, as soon as possible. The values of the

TABLE VI

Comparison Between Faraday and Poynting Methods in Estimating the Internal Flux Requirement (V·s) at SOFT for Different Plasma Scenarios

Case	1		3		6	
Model	Poynting	Faraday	Poynting	Faraday	Poynting	Faraday
$\Delta\Psi_{ind}$ (SOFT)	4.5	7.6	5.6	9.5	6.8	11.4
$\Delta\Psi_{res}$ (SOFT)	5.3	2.1	6.6	2.7	7.9	3.2
$\Delta\Psi_{int}$ (SOFT)	9.8	9.7	12.2	12.2	14.7	14.6

TABLE VII

Comparison Between Faraday Method and TSC in Estimating the Poloidal Flux Requirement (V·s) for Different Plasma Scenarios

Case	1		3		6	
Model	Faraday	TSC	Faraday	TSC	Faraday	TSC
$\Delta\Psi_{ind}$ (SOFT)	7.6	7.6	9.5	9.8	11.4	11.7
$\Delta\Psi_{res}$ (SOFT)	2.1	2.8[a]	2.7	2.9[a]	3.2	3.3[a]
$\Delta\Psi_{int}$ (SOFT)	9.7	10.4	12.2	12.7	14.6	15.0
$\Delta\Psi_{ext}(R_0)$ (SOFT)	11.5	11.4	14.4	14.2	17.3	17.1
$\Delta\Psi_p(R_0)$ (SOFT)	21.2	21.8	26.6	26.9	31.9	32.1
$\Delta\Psi_{ind}$ (EOFT)	10.2	10.5	12.4	12.3	12.7	12.8
$\Delta\Psi_{res}$ (EOFT)	4.6	5.3[a]	4.6	4.8[a]	3.5	3.6[a]
$\Delta\Psi_{int}$ (EOFT)	14.8	15.8	17.0	17.1	16.2	16.4
$\Delta\Psi_{ext}(R_0)$ (EOFT)	11.8	11.6	14.7	14.5	17.5	17.3
$\Delta\Psi_p(R_0)$ (EOFT)	26.6	27.4	31.7	31.6	33.7	33.7

[a]0.8 V·s added for the breakdown phase.[26]

TABLE VIII

Flux Requirement (V·s) for Flux-Minimizing Plasma Density Evolution

Case	1		3		6	
Model	Faraday	TSC	Faraday	TSC	Faraday	TSC
$\Delta\Psi_{ind}$ (EOFT)	10.2	10.5	12.4	12.3	12.7	12.8
$\Delta\Psi_{res}$ (EOFT)	4.6	4.6[a]	4.6	4.1[a]	3.5	2.9[a]
$\Delta\Psi_{int}$ (EOFT)	14.8	15.1	17.0	16.4	16.2	15.7
$\Delta\Psi_{ext}(R_0)$ (EOFT)	11.8	11.6	14.7	14.5	17.5	17.3
$\Delta\Psi_p(R_0)$ (EOFT)	26.6	26.7	31.7	30.9	33.7	33.0

[a]0.8 V·s added for the breakdown phase.[26]

plasma parameters at EOFT or ignition are the same as the ones reported in Tables II and III. Clearly, this procedure must allow an adequate current penetration rate to satisfy stability criteria and to guarantee a sufficient level of ohmic heating. The TSC estimates for cases 1, 3, and 6 with this flux-minimizing plasma density evolution are reported in Table VIII.

The values of $\Delta\Psi_p(R_0)$ reported in Table VIII are still lower than the maximum value of poloidal flux variation that can be delivered in R_0 by the PF system considered in the Ignitor design.[17]

IV.C. Engineering Requirement

One of the results of the TSC code is the time evolution of the current and voltage in all the coils for a particular plasma scenario. With this information, it is possible to verify the design of the PF system and, in particular, the capability of the transformer to deliver the necessary poloidal flux swing.

It is also possible to obtain, according to Eq. (15), the flux variation that must be delivered by the ohmic transformer, even if in a more qualitative way, by starting from the total poloidal flux requirement and then reducing this value by the contribution $\Delta\Psi_{vert}(R_0)$.

The plasma poloidal flux requirement at the plasma center $\Delta\Psi_p(R_0)$, the flux variation produced by the vertical field coils $\Delta\Psi_{vert}(R_0)$, and the flux variation that must be produced by the transformer at the plasma boundary $\Delta\Psi_{trans}(R_b)$ are reported in Table IX for the three reference plasma scenarios. The value of $\Delta\Psi_p(R_0)$ is obtained from TSC simulation, while $\Delta\Psi_{vert}(R_0)$ is calculated, according to our simplified model, by using Eq. (8) and the data reported in Tables I and II.

These results show that the most demanding scenario, in terms of the flux swing required by the transformer, is represented by both the 12-MA scenario and by the 10-MA plasma current discharge that does not

TABLE IX

Values of $\Delta\Psi_p(R_0)$, $\Delta\Psi_{vert}(R_0)$, and $\Delta\Psi_{trans}(R_b)$ (V·s) for Different Plasma Scenarios

	Case		
	1	3	6
$\Delta\Psi_p(R_0)$	26.7	30.9	33.0
$\Delta\Psi_{vert}(R_0)$	6.6	8.2	9.9
$\Delta\Psi_{trans}(R_b)$	20.1	22.7	23.1

reach ignition. This is not completely surprising if we take into account that even if the plasma current is larger in the 12-MA discharge,

1. ignition is reached early in the current flattop phase when the plasma current profile is still very broad (thus, a low inductive requirement)
2. the resistive requirement is lower because of the early ignition, the higher plasma temperature, and the larger bootstrap current fraction
3. the contribution of the vertical field is larger.

It may be useful to remember that a small reduction in the non-ohmic component (see C^{aux} in Table II) of the thermal diffusion coefficient[6] allows the 10-MA discharge (see case 5, Table II) to reach ohmic ignition with a reduction of 2.5 V·s compared with the value reported earlier.

IV.D. Evaluation of the Uncertainties

Here we try to estimate the uncertainties associated with the value of the poloidal flux requirement given earlier for case 3. To deal with this problem, it is easier to refer to the heuristic formulation of the problem given, for example, by the Faraday approach, since the uncertainties are related mainly to the internal component of the flux.

As far as the inductive part is concerned, the uncertainties are related to the variation of the flux inductance h_i. This problem assumes particular importance in a pulsed machine because, as has been shown by the results of the TSC simulation, the plasma current profile does not reach a steady-state, completely penetrated profile (see Fig. 3). Therefore, depending on the characteristics of the specific model used for the current diffusion process, different values of h_i can be obtained. By using the relationship between l_i and h_i [see Eqs. (58) and (59)], an upper boundary value for h_i can be estimated that takes into account empirical stability criteria, in the space $[q_\Psi(a), l_i]$, for density limit disruptions. In particular, based on the one determined in JET (Refs. 26, 27, and 28), the maximum allowable value of the Shafranov inductance is $l_i \leq 1.18$ for $q_\Psi(a) \simeq 3.5$. To this value of l_i corresponds a value of h_i that is ~12% higher than the one evaluated from the TSC simulation for case 3 and used in the evaluation of the poloidal flux requirement. Therefore, we assume an error of ~12% on $\Delta\Psi_{ind}$.

The external component (proportional to L_{ext} and M_{vert}) can be correctly evaluated, by means of a standard equilibrium code, once the plasma shape has been fixed. The relatively mild dependence of $L_{ext}(R_0)$ on the internal current distribution l_i and the plasma performance β_p can be evaluated in ~5% of $\Delta\Psi_{ext}(R_0)$ from Eq. (50), assuming that the maximum value of l_i is $\simeq 1.18$ and the maximum allowable value of β_p is $\simeq 0.3$. This boundary value of β_p is determined, in the Ignitor experiment, by the excitation of possible instability of global plasma modes with a dominant poloidal mode number $m^0 = 1$ (Ref. 5).

The error bar on the value of the Ejima coefficient and the lack of knowledge of the precise characteristics of the current rampup phase (in terms of the time evolution of parameters, such as the plasma peak density, the density profile peaking factor, the impurity level, the plasma shape, etc., that have influence on the plasma resistivity) are the sources of uncertainty in the resistive flux consumption. However, the experimental evidence[16] (JET, D-III, and JFT-2M) shows that high dI_ϕ/dt and high B_ϕ clearly reduce the resistive poloidal flux consumption, and thus, these values of the Ejima coefficient should be conservative for the Ignitor case. This fact is partially confirmed by the results reported in Table VIII, where it is shown that the heuristic models are in good agreement with the TSC code in case 1, while for higher dI_ϕ/dt and B_ϕ (cases 3 and 5), they predict a larger resistive poloidal flux requirement. We estimate that the uncertainty in the characteristics of the current ramp is of the order of the savings that were found as a result of changing the plasma density evolution ($\simeq 1.0$ V·s, corresponding to ~20% of $\Delta\Psi_{res}$). Therefore, the total uncertainty in the internal poloidal flux requirement $\Delta\Psi_{unc}$ for case 3 should be of the order of 14% of $\Delta\Psi_{trans}(R_b)$ (i.e., $\Delta\Psi_{unc} \simeq 3.2$ V·s).

Assuming that this estimate of the uncertainty is also correct for the other two cases (1 and 6), and adding this correction to $\Delta\Psi_{trans}(R_b)$, we obtain, as shown in Table X, the maximum magnetic flux variations,

$$\Delta\Psi^{max}_{trans}(R_b) = \Delta\Psi_{trans}(R_b) + \Delta\Psi_{unc} \ , \qquad (61)$$

that the ideal transformer must deliver for the three reference cases. Table X also reports the maximum magnetic flux changes that the PF coils must deliver at the plasma center:

$$\Delta\Psi^{max}_{c}(R_0) = \Delta\Psi^{max}_{trans}(R_b) + \Delta\Psi_{vert}(R_0) \ . \qquad (62)$$

V. SUMMARY AND CONCLUSIONS

A review of the formulation of the assessment of the poloidal flux requirement in a fusion experiment has been presented. Particular attention has been given

TABLE X

Values of the Maximum Poloidal Flux Requirement (V·s) for Different Plasma Scenarios

	Case		
	1	3	6
$\Delta\Psi_{unc}$	2.8	3.2	3.2
$\Delta\Psi_{trans}^{max}(R_b)$	22.9	25.9	26.3
$\Delta\Psi_{c}^{max}(R_0)$	29.5	34.1	36.2

to the derivation of the poloidal flux balance equation and to the interpretation of all the terms involved. It has been shown that if the total poloidal magnetic field is used, then the balance equation between poloidal flux consumed by the plasma and poloidal flux delivered by the poloidal field coils is correctly written at the plasma boundary. From this equation, the value of the poloidal flux that must be supplied at the plasma center is easily inferred by adding, to both sides of the balance equation, the poloidal flux variation produced by the coils between the plasma boundary and the plasma center.

Simple heuristic or analytic expressions that allow the evaluation of the internal (inductive plus resistive) and external poloidal flux consumption have been reported and applied to several plasma scenarios foreseen for a specific tokamak experiment (Ignitor). Equilibrium (TEQ) and transport (TSC) codes have been used to check the previous results. The agreement is fairly good. In particular, it has been shown that the value of the total poloidal flux requirement obtained with the heuristic and analytic expressions differ from the value estimated following the time evolution of the plasma discharge with the TSC code by an amount that is lower than the uncertainties associated with the evolution of the current density profile. Therefore, simple analytical expressions can be used in the first approximation to estimate the poloidal flux requirement, while numerical simulations of the plasma current penetration process are required to correctly evaluate and optimize the resistive flux consumption. This could be achieved by means of controlling the plasma density evolution, the variation of the plasma current ramp rate, the application of external heating, and the use of noninductive current drive techniques.

ACKNOWLEDGMENTS

It is a pleasure to thank B. Coppi for suggesting this problem, N. Pomphrey and L. E. Sugiyama for useful discussions on the subject, and S. C. Jardin, C. Kessel, and N. Pomphrey for their continuous support on the TSC code. Many thanks are due the referees for valuable comments and corrections. This work was sponsored in part by the U.S. Department of Energy and in part by ENEA of Italy under contract 91/58/IC111/88.

REFERENCES

1. B. COPPI, "High Current Density Tritium Burner," PRR-75/18, Massachusetts Institute of Technology (1975) and *Comm. Plasma Phys. Cont. Fusion*, **3**, 2 (1977).

2. "Ignitor Project Feasibility Study," ENEA (1989).

3. B. COPPI et al., "Current Density Transport, Confinement and Fusion Burn Conditions," *Proc. 13th Int. Conf. Plasma Physics and Controlled Nuclear Fusion Research*, Washington, D.C., 1990, Vol. 2, p. 337, International Atomic Energy Agency (1991).

4. L. E. SUGIYAMA and M. NASSI, "Free Boundary Current Ramp and Current Profile Control in a D-T Ignition Experiment," *Nucl. Fusion*, **32**, 387 (1992).

5. B. COPPI, M. NASSI, and L. E. SUGIYAMA, "Physics Basis for Compact Ignition Experiments," *Phys. Scripta*, **45**, 112 (1992).

6. B. COPPI et al., "Reconnection and Transport in High Temperature Regimes," *Proc. 14th Int. Conf. Plasma Physics and Controlled Nuclear Fusion Research*, Wurzburg, Germany, 1992, paper IAEA-CN-56/D-3-1(C), International Atomic Energy Agency.

7. S. C. JARDIN, N. POMPHREY, and J. DELUCIA, "Dynamic Modelling of Transport and Positional Control of Tokamaks," *J. Comput. Phys.*, **66**, 481 (1986).

8. W. A. HOULBERG, S. E. ATTENBERGER, and L. L. LAO, "Computational Methods in Tokamak Transport," ORNL/TM-8193, Oak Ridge National Laboratory (1982).

9. L. D. PEARLSTEIN, Lawrence Livermore National Laboratory, Private Communication (1992).

10. S. P. HIRSHMAN and G. H. NEILSON, "External Inductance of an Axisymmetric Plasma," *Phys. Fluids*, **29**, 790 (1986).

11. G. H. NEILSON and N. POMPHREY, "Use of Hirshman/Neilson External Inductance," Memorandum 93-921013-PPPL, Princeton Plasma Physics Laboratory (Oct. 1992).

12. S. EJIMA et al., "Volt-Second Analysis and Consumption in Doublet III Plasmas," *Nucl. Fusion*, **22**, 1313 (1982).

13. R. J. HAWRYLUK, K. BOL, and D. JOHNSON, "Volt-Second Consumption During the Start-Up Phase of PLT," *Nucl. Fusion*, **19**, 1519 (1979).

14. W. A. HOULBERG, "Volt-Second Consumption in Tokamaks with Sawtooth Activity," *Nucl. Fusion*, **27**, 1009 (1987).

15. J. T. HOGAN and T. S. TAYLOR, "Preliminary Analysis of DIII-D Volt-Second Consumption," Progress Report PH11-U2, ITER R and D Program (Oct. 1989).

16. P. LOMAS,"Scaling of Volt-sec Consumption During Inductive Current Ramp Up," Progress Report PH11-E1, ITER Physics R and D Program (Oct. 1989).

17. B. COPPI, M. NASSI, and the IGNITOR PROJECT GROUP, "Physics Criteria and Design Solutions for an Advanced Ignition Experiment," *Proc. 17th Symp. Fusion Technology*, Rome, Italy, 1992, paper V 09.

18. B. COPPI and E. MAZZUCATO, "Transport of Electron Thermal Energy in High Temperature Plasmas," *Phys. Rev. Lett. A*, **71**, 337 (1979).

19. O. GRUBER, "Scaling of Plasma Transport in Ohmically Heated Tokamaks," *Nucl. Fusion*, **22**, 1349 (1982).

20. B. COPPI and G. REWOLDT, "New Trapped-Electron Instability," *Phys. Rev. Lett.*, **33**, 1329 (1974).

21. B. COPPI and F. PEGORARO, "Theory of the Ubiquitous Mode," *Nucl. Fusion*, **17**, 969 (1977).

22. B. COPPI et al.,"Drift Instability Due to Impurity Ions," *Phys. Rev. Lett.*, **17**, 377 (1966).

23. C. S. CHANG and F. L. HINTON, "Effect of Impurity Particles on the Finite-Aspect Ratio Neoclassical Ion Thermal Conductivity in a Tokamak," *Phys. Fluids*, **29**, 3314 (1986).

24. M. E. MAUEL et al., "Achieving High Fusion Reactivity in High Poloidal Beta Discharges in TFTR," *Proc. 14th Int. Conf. Plasma Physics and Controlled Nuclear Fusion Research*, Wurzburg, Germany, 1992, paper IAEA-CN-56/A-III-4, International Atomic Energy Agency.

25. S. EJIMA et al., "Volt-Second Consumption in the DIII-D Tokamak," *Bull. Am. Phys. Soc.*, **31**, 1536 (1986).

26. P. J. LOMAS, B. J. GREEN, J. HOW, and JET TEAM, "High Current Operation in JET," *Bull. Am. Phys. Soc.*, **32**, 1837 (1987).

27. J. A. SNIPES et al., "Large Amplitude Quasi-Stationary MHD Modes in JET," *Nucl. Fusion*, **28**, 1085 (1988).

28. D. J.CAMPBELL et al., "Plasma Resistivity and Field Penetration in JET," *Nucl. Fusion*, **28**, 981 (1988).